Water Research 215 (2022) 118240

Contents lists available at ScienceDirect

Water Research

journal homepage: www.elsevier.com/locate/watres

Photoelectrocatalytic inactivation mechanism of E. coli DH5α (TET) and synergistic degradation of corresponding antibiotics in water

Zhenlian Qi [a,b], Guiying Li [a,b], Miao Wang [a,b], Chunliang Chen [a,b], Zhe Xu [a,b], Taicheng An [a,b,*]

[a] Guangdong Key Laboratory of Environmental Catalysis and Health Risk Control, Guangdong-Hong Kong-Macao Joint Laboratory for Contaminants Exposure and Health, Institute of Environmental Health and Pollution Control, Guangdong University of Technology, Guangzhou 510006, China
[b] Guangdong Engineering Technology Research Center for Photocatalytic Technology Integration and Equipment, Guangzhou Key Laboratory of Environmental Catalysis and Pollution Control, School of Environmental Science and Engineering, Guangdong University of Technology, Guangzhou 510006, China

ARTICLE INFO

Keywords:
Photoeletrocatalytic technology
Coexistence of ARB/ARGs with antibiotics
Bacteria inactivation
Antibiotic degradation
Synergetic mechanism

ABSTRACT

The occurrence and proliferation of antibiotic-resistance genes (ARGs) / antibiotic-resistant bacteria (ARB) have been currently aggravating due to the increase of antibiotic residues in the aquatic environment. The interaction of ARB/ARGs with antibiotics inevitably occurred during water purification, yet their synergistic purification mechanism remains unclear. Herein, a systematic approach was developed to understand, in-depth, the synergistic mechanism in the coexisted *E. coli* DH5α (TET) inactivation and tetracycline hydrochloride (TET) degradation using photoelectrocatalysis (PEC) as a model technology. Results showed that low dosage (0 – 40 ppm) of TET exerted a negative influence on ARB inactivation with prolonged bactericidal time from 60 to 160 min. Addition of TET in environmental concentration (5 – 60 ppm) resulted in sub-lethal damage and prolonged PEC treatment time (100 – 160 min), accounting for inhibition effects on ARB inactivation. The major reactive species (RSs) involved in ARB inactivation and TET degradation were evidenced as photogenerated hole, $^{\bullet}OH$ and $O_2^{\bullet-}$, whereas hole and $O_2^{\bullet-}$ were demonstrated to be the major disinfectants for ARB/ARG inactivation. The bacterial defense system displayed increased antioxidative activities of superoxide dismutase (SOD) and glutathione peroxidase (GSH-Px) to protect ARB cells against oxidative stress. Exposure to 60 ppm TET was a threshold where certain ARB cells were induced into viable but nonculturable bacterial cell (VBNC) state, as evidenced by plate counting and ATP activity analysis, together with the integral cell membranes observed by flow cytometry (FCM) and scanning electron microscope (SEM). These findings appeal for appropriate technical adjustments for water and wastewater treatment to ensure safety of water.

1. Introduction

The occurrence and proliferation of antibiotic-resistance genes (ARGs) / antibiotic-resistant bacteria (ARB) are gradually evolving into a global problem (Rodriguez-Rojas et al., 2013). Especially in the special period such as COVID-19 outbreak, the propagation of ARB/ARGs through sewage channels will be aggravated, seriously endangering the ecological environment and human health (Bhowmick et al., 2020; Daraei et al., 2020; Horn et al., 2020; Qu et al., 2020). It was reported that antibiotic residues, even at trace levels, potentially foster the antibiotic resistance and promote the proliferation of ARB/ARGs as an undesirable side-effect (Ghernaout and Elboughdiri, 2020; Jia et al., 2011). Unfortunately, antibiotic residues ubiquitously coexist with ARB/ARGs in aquatic environment, for example medical wastewater or sewage water. The consumed antibiotics with 48% being used for humans and the rest for animals are hardly completely metabolized in bodies, resulting in antibiotic residues (e.g. erythromycin, oxytetracycline) with detected levels ranging from tens of ng/L to hundreds of μg/L in the aquatic environments (Carvalho and Santos, 2016; Daghrir and Drogui, 2013; Jia et al., 2011; Kovalakova et al., 2020; Kümmerer, 2009). In medical wastewater, the level of antibiotic residues even hits hundreds of mg/L (Bansal, 2019). They pose intensifying concerns to trigger the increase in resistant strains of microorganisms worldwide and bring out particularly high risk of ARB/ARGs (Andreozzi et al., 2004; Besse and Garric, 2008). In this context, the development of safe and effective technologies has become an imperative need to simultaneously eliminate the coexisted ARB/ARGs and antibiotics from aquatic environment.

The wastewater treatment plants play the central role in regulating

* Corresponding author.
E-mail address: antc99@gdut.edu.cn (T. An).

https://doi.org/10.1016/j.watres.2022.118240
Received 25 January 2022; Received in revised form 23 February 2022; Accepted 27 February 2022
Available online 1 March 2022

the migration of ARB/ARGs and antibiotics from wastewater to the natural environment. Several light-driven advanced oxidation processes, such as photocatalysis (PC) and photoelectrocatalysis (PEC), have been reported in literature or already applied in water purification of ARB/ARGs and antibiotics (Liu et al., 2021; Meng et al., 2010). Noted that PEC as a promising method has attracted quite a lot attention in the inactivation of ARB/ARGs or antibiotics degradation separately in recent years (Qin et al., 2021; Shi et al., 2020). PEC have shown effective inactivation capacity to a variety of bacteria, such as *Escherichia coli* and *Staphylococcus aureus* (Li et al., 2011; Lin et al., 2021; Nie et al., 2014; Sun et al., 2014), and even can inactive ARB/ARGs, such as tetracycline-resistant bacteria and β-lactame-resistant bacteria (Cai et al., 2021; Jiang et al., 2017; Yin et al., 2019; Yin et al., 2021). However, PEC was generally applied to inactivate ARB/ARGs in the absence of antibiotics, which faced a large gap from the real situation of the co-existed ARB/ARGs and antibiotics in many complex water systems. It was demonstrated that antibiotics such as tetracycline (TET) and ofloxacin were degraded by photogenerated holes (h^+) and reactive oxidation species (ROSs) in PEC system (Li et al., 2014; Li et al., 2012; Meng et al., 2010; Ye et al., 2021), which might bring about negative influence on inactivation of ARB/ARGs. Besides, exposure to several adverse stressors, such as antibiotic residues and oxidative stimulus, may induce a synergistic reinforcement to accelerate bacterial death or stimulate various stress responses inside living cells to protect bacteria from damage and death (Cai et al., 2021; Ghernaout and Elboughdiri, 2020; Jiang et al., 2017; Li et al., 2013), which would make the inactivation process aberrant complicated. Therefore, in-depth understanding photoelectrocatalytic inactivation mechanism of various ARB/ARGs and synergistic degradation of antibiotics in a complex water system by PEC is highly required but there is still a lack of relevant reports.

The aims of the current study are, therefore, to 1) identify the dominant species of ARB/ARG inactivation and antibiotic degradation within these coexisted water system; 2) verify the relationship between RSs level, antioxidant enzyme activities and ARB/ARG inactivation efficiencies; 3) unveil the changes in cell membrane integrity, cell morphology and ARG abundance utilizing flow cytometry (FCM), field-emission scanning electron microscopy (FESEM) and real-time polymerase chain reaction (RT-PCR) during PEC processes; 4) clarify possible synergistic purification mechanism of ARB/ARGs and antibiotics during PEC processes.

2. Materials and methods

2.1. Materials

All the chemicals were of reagent grade and used as-received. Ultrapure deionized water (> 18 MΩ cm), produced with a Milli-Q water purification system, was used to prepare all the experimental solutions. Antibiotic-resistant bacterial strain related to tetracycline hydrochloride (TET) namely *E. coli* DH5α (TET) and antibiotic TET, were selected as the treated objects.

2.2. PEC apparatus setup

A cylindrical glass PEC reactor (50 mL volume) with a quartz window for UVA illumination was used to perform synchronous ARB/ARG inactivation and antibiotic degradation experiments, using a two-electrode system with a TiO_2 nanotube array photoanode and a platinum foil counter electrode. A voltage of 1 V was applied to the two-electrode system by a direct current power supply (HSPY-36–03, China) and a LED lamp with maximum emission at 365 nm (100 mW/cm^2) was used to provide the UV light source. The reaction temperature was controlled in 25 °C ± 2 °C and the reaction solution was mixed with a constant temperature digital magnetic stirrer. For each run of PEC process, 50 mL 0.20 M $NaNO_3$ solution containing 1×10^8 colony forming unit per milliliter (CFU/mL) *E. coli* DH5α (TET) and antibiotic TET of specified concentrations, were added into the reactor, and aliquots of solution were withdrawn at constant time intervals during PEC, and then were processed into samples for further measurements.

2.3. Quantification of ARB viability and TET degradation

The *E. coli* DH5α (TET) strain was constructed by our research group, which contains an ARG-encoded plasmid conferring resistance to TET (Yin et al., 2020). The minimum inhibitory concentration (MIC) of TET against *E. coli* DH5α (TET) was tested in the range of 256 – 512 ppm through two-fold dilutions in 96-well plates. The bacterial cells were cultured in the nutrient broth growth medium at 37 °C for 16 h so that the logarithmic phase of bacterial growth was reached. The cultured bacteria were washed with sterilized 0.2 M $NaNO_3$ via centrifugation. Then the bacterial cell concentration was adjusted to a final cell concentration of 1×10^8 CFU/mL in 0.2 M $NaNO_3$ solution, which base on the principle that the bacteria need persist appropriate osmotic pressure during PEC. For each obtained bacterial sample, an appropriate gradient dilution was conducted with sterilized 0.9% NaCl solution and 0.1 mL diluted sample was uniformly spread on nutrient agar plates in triplicate, and then the nutrient agar plates were incubated for 24 h at 37 °C. The number of single colonies formed was counted to quantify the viable and cultivable bacterial cells.

The concentration of TET was measured with High Performance Liquid Chromatography (HPLC) with chromatography column Athena C18-WP (4.6 mm × 150 mm, 5 μm), and the mobile phase was consisted of water containing 0.1% v/v formic acid (A) and methanol (B). The degradation intermediates of TET were analyzed using Ultra-performance liquid chromatography coupled to hybrid Quadrupole-Exactive Orbitrap mass spectrometry (UHPLC-Q-Orbitrap HRMS) (Thermo Scientic™ Dionex U3000), and the base peak intensity chromatographic data obtained in both ESI positive and negative modes. Full scan spectra were measured range from 150 to 2000 *m/z*. The chromatography column was Waters ACQUITY UPLC® BEHC18 (2.1 mm × 100 mm, 1.7 μm) and the column temperature was 35 °C. A quaternary pump was used, and the mobile phase was consisted of water containing 0.1% v/v formic acid (A) and methanol (B) with gradient elution. The flow rate was set at 0.25 mL/min and the injection volume was 2 μL for each analysis. All the data acquired would be processed in the Thermo Xcalibur™ data system version 4.1. Detailed information is summed in Table S1 in Supporting Information (SI).

2.4. Assay of extracellular and intracellular ROS level

The levels of the ROSs in water generated during PEC process was analyzed with electron spin resonance measurements (ESR, EMXplus™, Bruker Biospin). In the first ten minutes of PEC running, ESR spectra of $^{\bullet}OH$ and $O_2^{\bullet-}$ were trapped by DMPO in aqueous dispersion and in methanol dispersion, respectively. ESR spectrum of $^1O_2$ was trapped by TEMP in aqueous dispersion.

To explore the oxidative stress levels of bacteria, the levels of intracellular ROSs in the *E. coli* DH5α (TET) cells were also detected during PEC process with different TET concentrations variation. Briefly, the intracellular ROSs were indirectly quantified using a probe of fluorogenic dye 2′7′-dichlorofluorescein diacetate (DCFH-DA). DCFH-DA can freely go through the cell membrane with no fluorescence. After entering cell, DCFH-DA can be hydrolyzed by intracellular esterase to produce dichlorodihydrofluorescein diacetate (DCFH), which cannot penetrate the cell membrane, making it easy for the probe to be loaded into the cell. The intracellular ROSs can oxidize non-fluorescent DCFH to produce fluorescent dichlorofluorescein (DCF), and the level of ROSs in the bacterial cells can be determined by detecting the fluorescence of the DCF. Detailed experimental procedures are described in the SI.

2.5. Assay of antioxidant enzyme activities and respiration rate of bacteria

The activities of various antioxidant enzymes, including catalase (CAT), superoxide dismutase (SOD), and glutathione peroxidase (GSH-Px), that can reduce intracellular peroxidation levels, were also tested. Briefly, the total protein of bacterial cell suspension in each sample was extracted with the Bacterial Protein Extraction Kit (C600596, Sangon Biotech, China). The protein samples extracted were analyzed for SOD, CAT and GSH-Px activities using Total Superoxide Dismutase Assay Kit with WST-8 (S0101S, Beyotime Biotechnology, China), Catalase Assay Kit (S0051, Beyotime Biotechnology, China) and Cellular Glutathione Peroxidase Assay Kit with NADPH (S0056, Beyotime Biotechnology, China), respectively. The cellular adenosine-triphosphate (ATP) concentration of bacterial cell suspension in each sample was measured using ATP Assay Kit (S0026, Beyotime Biotechnology, China).

2.6. Evaluation of cell membrane permeability and integrity

The permeability and integrity of bacterial membrane were assessed by FCM (BD FACSAria II, BD Biosciences). Briefly, the bacterial suspension of each sample obtained was diluted into 10^6 – 10^7 CFU/mL and immediately stained with SYTO-9 and Propidium iodide (PI) with LIVE/DEAD BacLight Bacterial Viability Kit (2,031,174, Invitrogen by Themo Fisher Scientific). SYTO-9 could stain all bacterial cells with green fluorescence while PI could stain destroyed or dead cells with red fluorescence. For completing the staining, samples were incubated with SYTO-9 and PI for 20 min at room temperature in the dark. Forward scatter (FSC) versus side scatter (SSC) biplots were used to identify and gate the bacterial population by filtering background particles and noise out. The green fluorescence of SYTO-9 and red fluorescence of PI were filtered on the FL1 channel (530/30 nm) and the FL3 channel (>670 nm long pass), respectively. For each sample, about 10,000 cells were collected and analyzed. All acquired date were processed using BD FACSDiva™ software 6.0.

2.7. The analysis of cell morphology

The cellular structure of *E. coli* DH5α (TET) sampled during different treatment intervals was observed by tungsten filament scanning electron microscope (SEM, S-3400 N, Hitachi, Japan). SEM analysis was conducted as follows: the bacterial cells were firstly fixed on a single crystal silicon with 2.5% glutaraldehyde solution for 2 h. After washing with sterilized PBS solution for three times, the samples were dehydrated with a graded series of ethanol (30%, 50%, 70%, 90%, and 100%) for 10 min, respectively. Finally, the dehydrated samples were dried by vacuum freeze drying, coated with gold foil, and observed under SEM.

2.8. Evaluation of gene abundance related TET resistance and oxidative stress

Total DNA of each sample obtained was extracted with Ezup Column Bacteria Genomic DNA Purification Kit (B518255, Sangon Biotech, China). Quantification of 23 typical genes related TET resistance and oxidative stress found in nature were carried out using real-time polymerase chain reaction (RT-PCR). The 16S rRNA gene as an amplification internal control was also evaluated by RT-PCR, and detailed information about recipes and primers for RT-PCR is in Table S2 in SI. All the data expressed in this study were replicated in triplicate.

3. Results and discussion

3.1. ARB inactivation under antibiotics with different concentrations

To determine the PEC inactivation activity under the coexistence of ARB cells and antibiotics, time-killing curves were firstly plotted using plate counting method for PEC inactivation of ARB (*E. coli* DH5a (TET)) under TET in a concentration range of 0 to 360 ppm (Fig. 1a). Complete bacterial inactivation was obtained within 60 min in the absence of TET, suggesting PEC alone can effectively inactivate ARB cells with a concentration of 10^8 CFU/mL and also confirmed by our early study (Nie et al., 2014). It was also observed that low dosage of TET exerted a negative influence on ARB inactivation. Increasing TET concentration from 5 to 40 ppm resulted in prolonged PEC inactivation time from 100 to 160 min (Fig. 1a), where the removal of TET was accelerated with a proximately 80% removal efficiency achieved (Fig. 1b). Surprisingly, a synergistic effect between bacteria inactivation and antibiotics degradation occurred when the dosage of TET was up to 60 ppm, which significantly facilitated the inactivation of ARB with a complete inactivation within 120 min and slowed down TET removal efficiency (Fig. 1a and b). However, adding 120 and 360 ppm TET alone also resulted in a certain amount of inactivation of ARB (Fig. 1c), exactly the same as the previous results in Fig. 1a. This provided evidence that the bactericidal effect of PEC would be deemed less important in the presence of TET higher than 120 ppm and antibiotics may inactivate bacteria more quickly than PECs at high antibiotics concentration (Wang and Zhuan, 2020; Wu and Hu, 2020). Therefore, 0 – 60 ppm of TET was used in the following experiments to elucidate the synergistic purification effect of PEC system in bacteria and TET coexisted water system.

3.2. Relative contributions of ROSs

During PEC process, the photogenerated holes could oxidize the adsorbed surface water molecules and hydroxyls into $^{\bullet}OH$, then the photogenerated electrons react with O_2 to produce $O_2^{\bullet-}$ (Li et al., 2012; Meng et al., 2010). It is generally accepted that the main active substances in PEC process are holes, $^{\bullet}OH$, $O_2^{\bullet-}$ that are able to strongly attack various pollutants (Li et al., 2012; Wang and Zhuan, 2020). To illuminate the possible main ROSs involved in ARB inactivation and TET degradation except for the part directly oxidized by holes on the photoanode surface, the ESR spin-trap experiments were used to also identify the relative contribution of other ROSs except photogenerated holes including $^{\bullet}OH$, $O_2^{\bullet-}$ and $^1O_2$ in PEC process by the ROSs scavenging method descript in our early works (Cai et al., 2020; Wang and Zhuan, 2020). The obvious signals of DMPO-$^{\bullet}OH$ (Fig. 2a) and DMPO—$O_2^{\bullet-}$ (Fig. 2b) indicated that large quantities of $^{\bullet}OH$ and $O_2^{\bullet-}$ were both generated in PEC system (Mousset and Dionysiou, 2020). With the addition of 20 ppm TET, the characteristic peaks of DMPO-$^{\bullet}OH$ and DMPO—$O_2^{\bullet-}$ were substantially weakened, suggesting that both $^{\bullet}OH$ and $O_2^{\bullet-}$ were responsible for the degradation of TET except the direct contribution of photogenerated holes (Ma et al., 2019). In addition, the initially produced radical from the reaction between TET and $^{\bullet}OH$ may react with O_2 to release $O_2^{\bullet-}$, which may provide additional source of $O_2^{\bullet-}$ in the system. The observed weak peaks of TEMP-$^1O_2$ might be generated from the further oxidation of $O_2^{\bullet-}$ by photogenerated holes (Shi et al., 2022), whereas it completely vanished with the addition of TET (Fig. 2c). These results suggested the competitive consumption of $^{\bullet}OH$, $O_2^{\bullet-}$ and $^1O_2$ by increased TET, could partially account for the retarded inactivation of ARB in this coexisted system of ARB and antibiotics. Besides, considering the low concentration of $^{\bullet}OH$ and $^1O_2$ in the presence of TET, holes and $O_2^{\bullet-}$ were thereby believed as dominated RSs for inactivation of ARB and degradation of antibiotics within this PEC system.

3.3. Bacterial inactivation mechanism in the presence TET

3.3.1. Stress response under co-exposure to PEC and TET

The attacks by various RSs are usually an important pathway for ARB inactivation during PEC process. To further clarify the oxidative response of ARB in the presence of TET, the activities of intracellular ROSs and main antioxidant enzymes including SOD, GSH-Px and CAT, were monitored during PEC process with various concentrations of TET

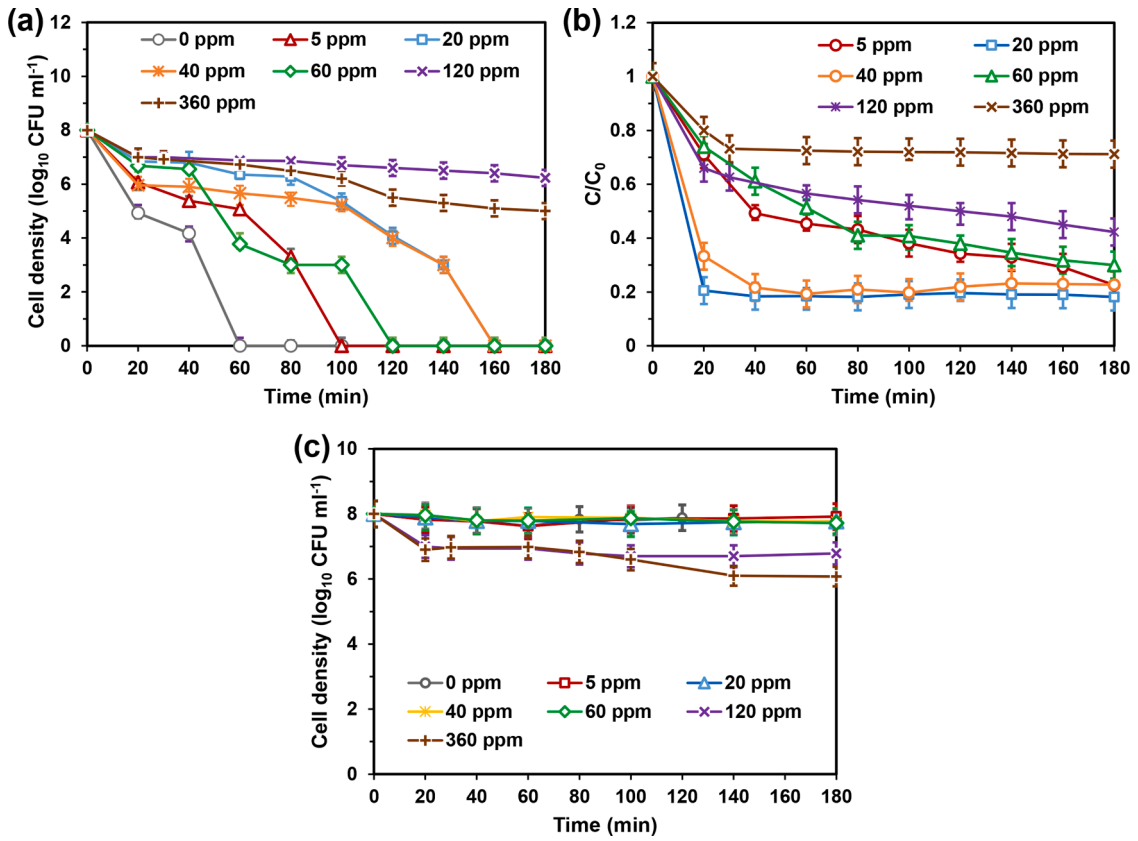

Fig. 1. PEC (a) inactivation of ARB and (b) removal of TET in the ARB and antibiotics coexisted water system, and (c) ARB inactivation by TET with different concentrations (0 – 360 ppm).

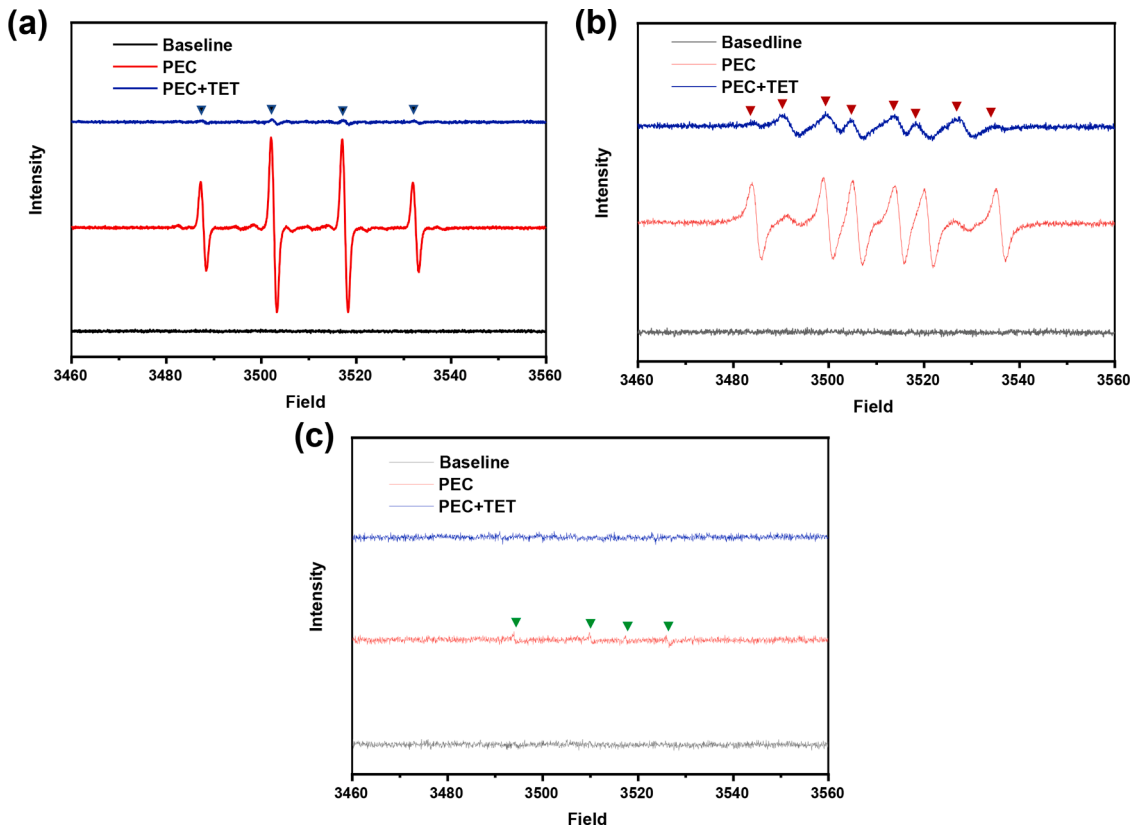

Fig. 2. Electron paramagnetic resonance (EPR) spectra of (a) DMPO-$^{\bullet}$OH, (b) DMPO- $O_2^{\bullet-}$, (c) TEMP-$^1O_2$ in PEC process in the presence/absence of TET (20 ppm).

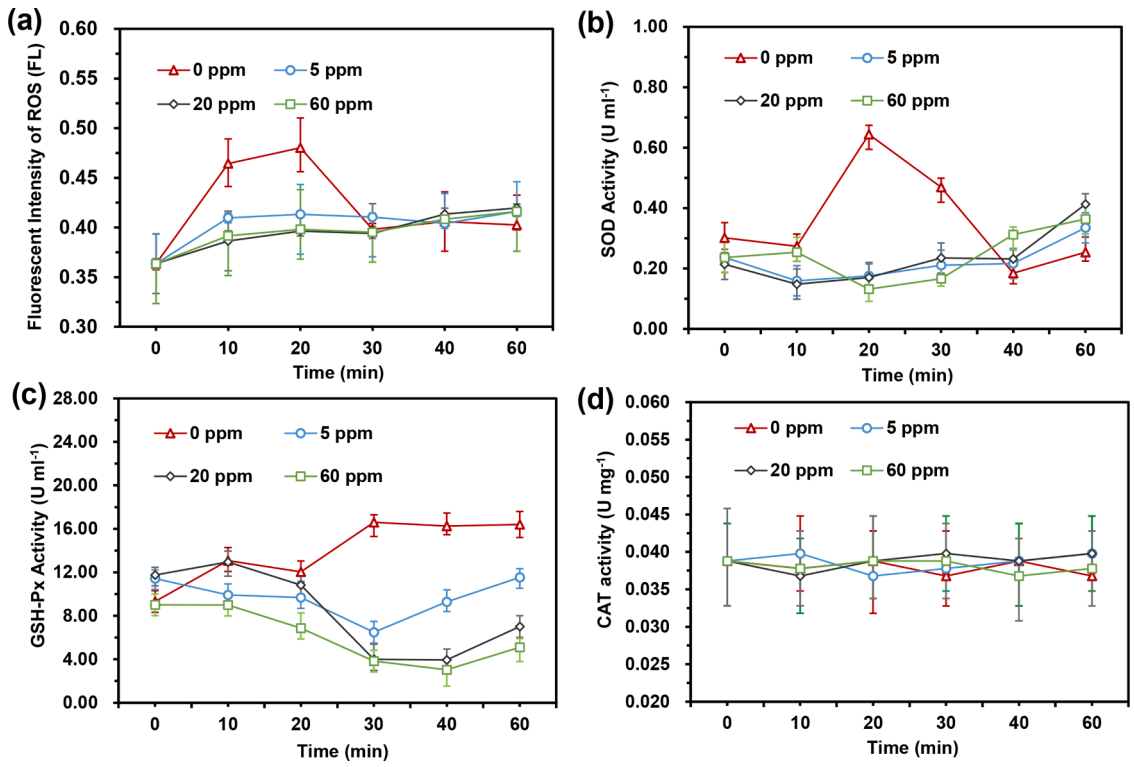

Fig. 3. Evolution of (a) intracellular ROS levels and antioxidation enzyme activities of (b) SOD, (c) CAT and (d) GSH-Px.

(Fig. 3). First of all, in the absence of TET, the intracellular ROS level was found to sharply increase at the beginning 20 min and then followed a quick decrease (Fig. 3a). This result, combined with the complete inactivation of ARB cells achieved within 60 min (Fig. 1a), suggested that PEC treatment alone could directly trigger bacterial oxidative stress systems and induce disruption of cellular redox equilibrium through quick raising accumulation of intracellular ROSs according to early references (Gusarov and Nudler, 2005; Yin et al., 2020). In contrast, the presence of TET (5 – 60 ppm) resulted in a low level of intracellular ROSs (Fig. 3a), suggesting the mitigated oxidative responses of ARB cells. This result matches well with the ESR results, further confirming that TET could act as a ROS scavenger to reduce the oxidative inactivation of ARB. The activity of SOD and CAT represents the response of bacteria toward $O_2^{\bullet-}$ and H_2O_2, respectively, while both H_2O_2 and lipid peroxides enable the stimulation of GSH-Px according to references (Djordjevic et al., 2004; Wilke et al., 1992). In Fig. 3b, the evolution of the SOD activity matched well with that of the intracellular ROSs concentration, implying that $O_2^{\bullet-}$ might be the main intracellular ROSs to attack the intracellular substances of the ARB. This speculation was also supported by previous studies where $^{\bullet}OH$ in solution was incapable to penetrate the bacterial membrane due to its short half-life and short half diffusion length (Sun et al., 2016; Sun et al., 2014). Noted that GSH-Px activities decreased slowly at the beginning and then increased gradually (Fig. 3c), while the CAT activities remained steady throughout 60 min of PEC treatment (Fig. 3d). Therefore, we can also conclude that bacterial defense system tended to display increased activities of SOD and GSH-Px to protect the ARB cells during PEC treatment alone. However, the observed increase in SOD and GSH-Px activities was negligible in the presence of TET. This observation, again, demonstrated the alleviated oxidative pressure of ARB by TET.

3.3.2. *Mechanisms of ARB inactivation in the presence TET*

The destruction of cell membrane integrity of bacteria was generally used as an indicator of the first step of the bactericidal effect (Pigeot-Remy et al., 2012; Sun et al., 2014). To characterize the integrity of ARB cell membrane under co-exposure to PEC and TET, the FCM of SYTO 9/PI-stained ARB cells were investigated according to early reference (Lindivat et al., 2020). As shown in Fig. 4a, a quadrant marker divided two-parameter plots into four quadrants (Q1, Q2, Q3 and Q4) to discriminate bacterial cells in different states: dead PI-stained cells (Q1), injured SYTO-9/PI double-stained cells (Q2), unstained cells (Q3), and viable SYTO-9-stained cells (Q4) based on the method reported in the reference (Lindivat et al., 2020). Before the exposure to PEC and TET, the FCM signals almost located in Q4 quadrant, suggesting nearly all the cells have the intact membranes and a very small fraction of injured cells before experimental operation (Fig. 4$a_{a1\text{-}d1}$). As displayed in Fig. 4a, the distribution of FCM signals intimately related on the concentration of TET. During the exposure to PEC alone, the proportion of membrane damaged cells increased to 97.1% in the first 60 min and 98.5% of 180 min (Fig. 4a_{a2}-a_{a3}). With low dosage (5–20 ppm) addition of TET, the proportion of membrane damaged cells decreased to 73.2% – 86.2% within 60 min whereas 97.6% was obtained within 180 min (Fig. 4a_{b2}-a_{b3}). Increasing TET concentration to 60 ppm, the proportion of damaged cells increased to 72.9% within 60 min. However, no membrane damage was identified as the treatment further extended to 180 min. This phenomenon suggested that excessive antibiotics residues might become dominated strategy to inactive bacteria rather than PEC in this coexisted water system of ARB and antibiotics (Fig. 4a_{c2}-a_{c3}).

It was of interest to find a great deviation between the ARB inactivation and membrane damage results (Fig. S1). Noted that the percentages of culturable viable cells measured by plate counting method were all more than 60% within 60 min of PEC treatment in the presence of 5 – 20 ppm TET, much higher than the damage percentage of cell membrane obtained by FCM analysis. These results suggested that a proportion of the membrane damaged cells remained culturable, which might be benefited from the bacterial self-defense and auto-repair mechanisms as previously reported (Schottroff et al., 2018; Withers, 1975; Zhao et al., 2013). By further increasing TET concentration to 60 ppm, distinctly higher percentage of the membrane damaged cells was observed using FCM method as compared with the results using plate counting method within 60 min, where certain cells remained intact membrane but cannot be cultured. According to previous studies, harsh

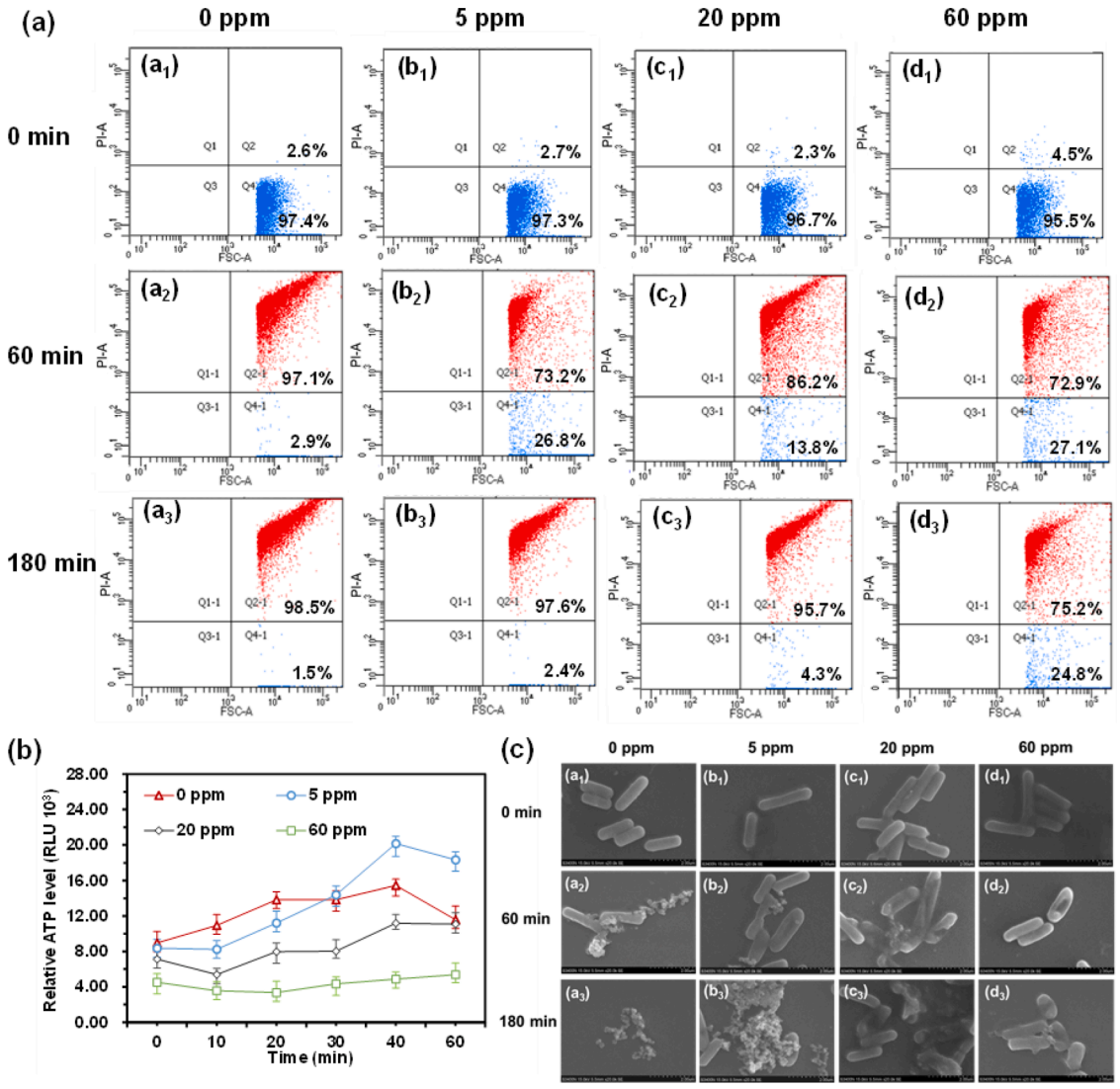

Fig. 4. (a) FCM images, (b) relative ATP level and (c) SEM of ARB cells at different PEC treatment time (0 min, 60 min, 180 min) in the presence of TET (0 – 60 ppm).

conditions can induce bacterial cells into viable but nonculturable (VBNC) state, in which the cells still keep intact membranes but lose the ability to form colonies (Ayrapetyan et al., 2015; Casini et al., 2018; Chen et al., 2018; Guo et al., 2020). Herein, our results suggest that excessive antibiotic restudies within certain concentration range in PEC system might also induce ARB turning into VBNC state. We speculate part of the reasons may be associated with the inhibition of ARB cell metabolism under co-exposure to PEC and TET (Merlin et al., 2011; Yin et al., 2019).

One major indicator of cell metabolic activity is the potential of the cells to produce ATP (Pu et al., 2019), thus, we herein also examined the relative ATP levels of ARB cells during PEC treatment in the presence of different dosages of TET (0 – 60 ppm) (Fig. 4b). With PEC treatment alone, the cellular ATP level showed a slight increase and followed a drop after 40 min. This result agreed with the changes in the activities of intracellular ROSs and SOD (Fig. 3a and 3b), further suggesting a correlation between metabolic activity and viability of bacterial cells (Barrette et al., 1989). The presence of 5 ppm TET triggered a higher cellular ATP level than that with PEC treatment alone, which might be resulted from the increased survival efficiency of ARB cells as shown in Fig. 1a. Addition of TET with a range of 20 – 60 ppm, the cellular ATP levels were inversely correlated with TET concentration and significantly lower than those of adding TET with a range of 0 – 5 ppm. This suggested that 20 – 60 ppm TET might facilitate some ARB cells into dormant state with low metabolism by decreasing ATP generation activities, in which ARB cells may gain a decreased cellular susceptibility to osmotic pressure and exhibit reduced cell membrane damaged effects to survive PEC treatment (Chen et al., 2018; Guo et al., 2020; Klein and Lewinson, 2011).

To directly observe the characteristic of cell membrane damage, SEM was also employed to image the morphologies of treated bacterial cells during PEC process with different dosages of TET. As shown in Fig. 4c_{a1}-c_{d1}, the untreated cells were solid rod shapes with intact and smooth membrane. After 60 min of PEC treatment, apparent crevasse yawned at cell membrane and significant leakage of intracellular substances were observed. Only large amount of bacterial cell debris remained after 180 min treatment. The SEM images clearly showed that the intensities of cell membrane destruction were dependent on the changes of cell membrane shape and fine structure over PEC treatment time. Increasing TET from 5 to 60 ppm, the cell membranes presented a reduced damage with fewer microstructures of depression, distortion, wrinkling and rupture after 60 min treatment (Fig. 4c_{a2}-c_{d2}), which was attributed to the quenched effect of TET. Throughout 180 min of PEC treatment in the presence of 60 ppm TET, some ARB cells became small, short and ellipsoidal with intact membranes (Fig. 4c_{a3}-c_{d3}), but they were complete inactivated and nonculturable as demonstrated by plate counting method (Fig. 1a). This suggested that increasing TET up to 60 ppm during PEC treatment may present VBNC-inducing conditions,

consistent well with FCM analysis.

3.3.3. Evaluation of gene abundance related TET resistance

To further investigate the inactivation and damage of ARGs, the relative abundance of typical genes related to TET resistance and oxidative stress were also examined during PEC treatment intervals (Jiang et al., 2017). With increasing TET from 0 to 60 ppm, the relative abundance of tested gene residues related to ribosomal protection proteins, efflux of TET and oxidative stress obviously increased (Fig. 5), which might be attributed to the alleviated oxidation damage of DNA by TET based on ROSs scavenger effects. In addition, low concentration of TET facilitated the inactivation of tested genes related to SOS response (Fig. 5), which is a basic function of the cells to survive in a stressful situation according to early references (Erental et al., 2014; Sutton et al., 2000). This might be explained by that SOS response appeared to be in repairing DNA lesions caused by oxidative stress under co-exposure to PEC and low dosage of TET, in which the related DNA would unwind the double helix and tend to be vulnerable to oxidative attacks (Janion, 2001; Sutton et al., 2000). However, with increasing TET concentration to 60 ppm, the relative abundance of tested genes residues related to TET resistance was observed considerably higher. This might be resulted from the increased amount of ARB cells in VBNC state as demonstrated in Fig. 4, leading to the retention of more active ARG residues and potential risk of their continued spread.

3.4. Degradation pathway of TET in the presence ARB

To further understand the degradation pathway of TET in the ARB/ARGs and antibiotics coexisted system, PEC degradation experiments of TET in the presence of ARB were also examined, and the UHPLC-Q-Orbitrap HRMS was employed to identify its degradation intermediates. The major intermediates and final products of TET degradation were identified and the MS characteristic of all TET degradation intermediates are all shown in Fig. S2 in SI. In summary, the degradation pathways of TET in the presence of ARB were grouped as three dominant routes as proposed in Fig. 6. In Route I, except TET (a), intermediate (b) (m/z = 477.1500) was identified as hydroxylation product of TET attacked by $^{\bullet}OH$, then the carbon-chain scission produced intermediate (e) (m/z = 396.8009) was obtained. With the further attacks by RSs, mainly holes, $^{\bullet}OH$ and $O_2^{\bullet-}$, intermediate (e) opened the benzene ring to produce intermediates (h) (m/z = 351.2492) and (l) (m/z = 242.2838). In Route II, intermediate (c) (m/z = 461.1552) was another hydroxylation product of TET attacked by $^{\bullet}OH$, then, the N-methyl group was oxidized to the carbonyl group, intermediate (f) (m/z = 509.1395) was formed. With the further attacks by ROSs, intermediate (f) opened the benzene ring to produce intermediates (i) (m/z = 451.0993) and (l) (m/z = 242.2838). In Route III, intermediate (d) (m/z = 399.1546) was formed from TET through N and C demethylation reaction. ROSs further attacked intermediate (d) with loss of NH_2 and ring-opening reaction to produce intermediates (g) (m/z = 432.2798), (j) (m/z = 403.2490), (k) (m/z = 367.2186), and (l) (m/z = 242.2838). Although intermediates (h), (k), and (l) still have the potential for further degradation in a sufficient time of PEC treatment, but some intermediates like those with m/z = 461, 432 and 477 may retain some kind of toxicity according to the early references (Khan et al., 2010; Wang et al., 2018), which might present additional stressor to induce the ARB cells entering VBNC state as a survival strategy and the decrease in the inactivation of ARGs. This is worth further study to systematically analyze the influence of degradation intermediates on the inactivation and propagation of ARB/ARGs during PEC treatment.

4. Conclusions

This study mainly presented an in-depth understanding of the synergistic mechanism of the inactivation of *E. coli* DH5α (TET) bacteria and the degradation of corresponding antibiotics (TET) in coexisted water system using PEC as a model technology. The results demonstrated that PEC treatment alone quick inactivated ARB/ARGs by raising accumulation of intracellular ROSs and disrupting the cellular redox equilibrium. Meanwhile, the bacterial defense system tended to increase antioxidative activities of SOD and GSH-Px to protect ARB cells against the oxidative stress. The addition of TET in water system of bacteria inhibited the inactivation of ARB/ARGs mainly due to competing for the reactive species such as hole, $^{\bullet}OH$ and $O_2^{\bullet-}$, whereas the ARB/ARG

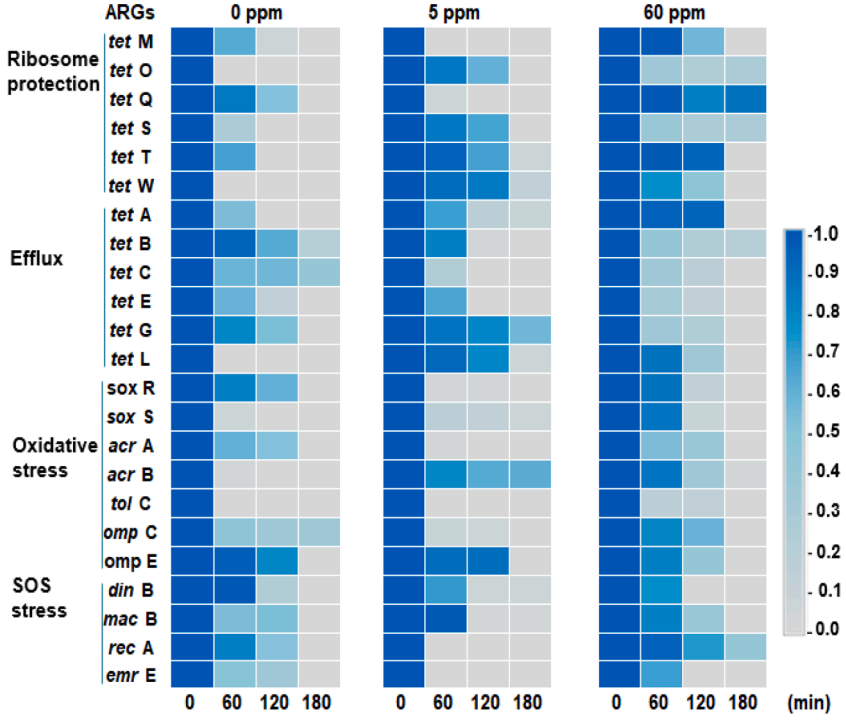

Fig. 5. Elimination of typical genes related TET resistance and oxidative stress during PEC treatment with different dosages of TET (0 – 60 ppm).

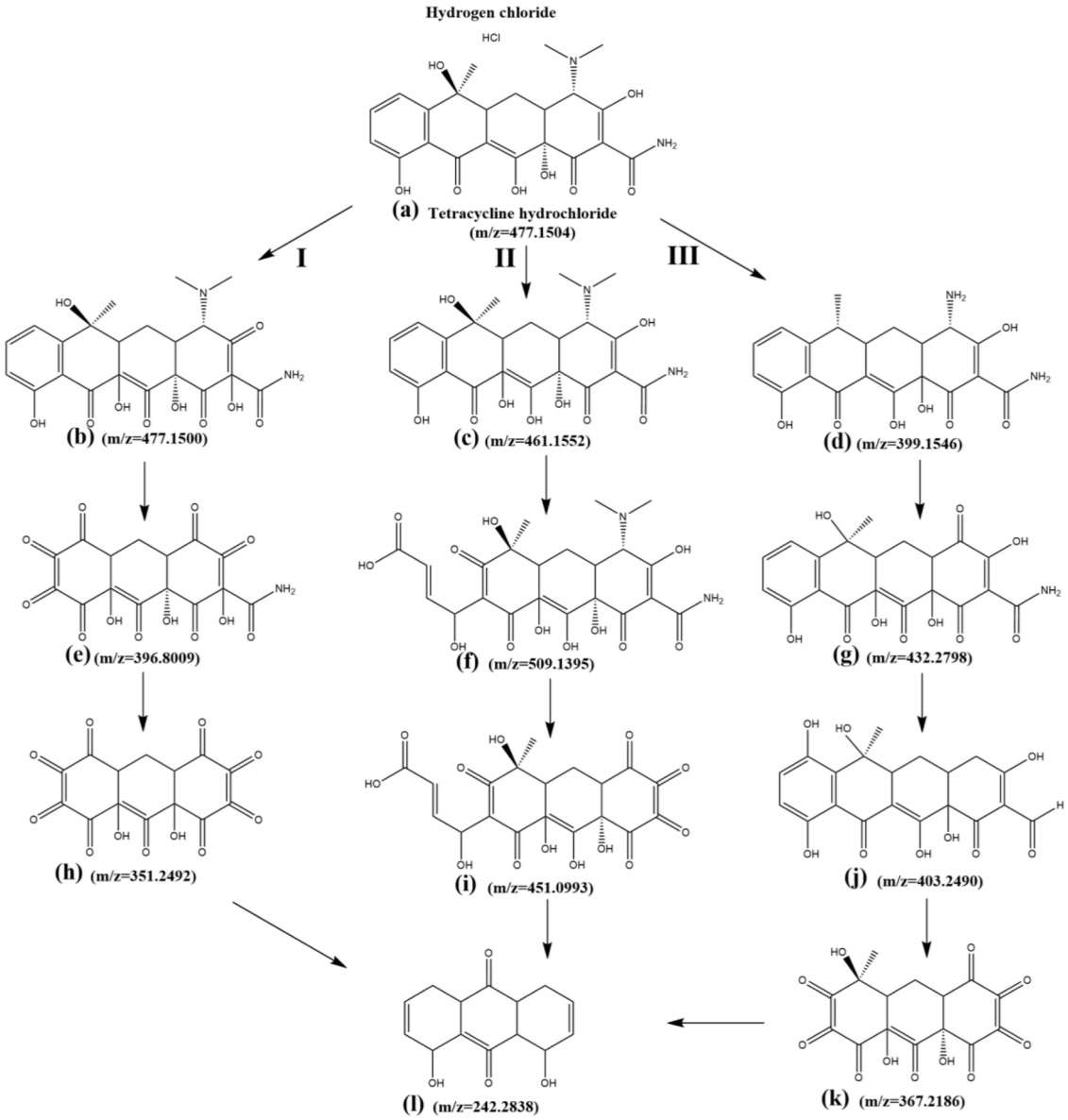

Fig. 6. Proposed degradation pathway of TET in the presence of ARB.

inactivation was dominated by holes and $O_2^{\bullet -}$. Of particular concern is that the exposure of PEC together with TET may facilitate some ARB cells turning into VBNCs, leading to the retention of more active ARG residues and potential risk of their continued spread. Although some aspects remain unclear and the studied system is a typical example in real time, the evaluation of synergistic mechanisms of ARB/ARG inactivation and antibiotic degradation is a task worthy of a more complete and exhaustive approach to help avoid underestimating the risk of antibiotic resistance spread into the environment.

Appendix A. Supplementary data

Supplementary data associated with this article can be found, in the online version.

Declaration of Competing Interest

The author declare that they have no known competing financial interests or personal relationships that could have appeared to influence the work reported in this paper.

Acknowledgements

This work was supported by the Guangdong Provincial Key R&D Program (2020B1111350002), National Natural Science Foundation of China (U1901210, 41573086, and 42077333), Key Project of Guangdong-Guangxi Joint Fund (20202011040000070), and Local Innovative and Research Teams Project of Guangdong Pearl River Talents Program (2017BT01Z032).

Supplementary materials

Supplementary material associated with this article can be found, in the online version, at doi:10.1016/j.watres.2022.118240.

References

Andreozzi, R., Caprio, V., Ciniglia, C., de Champdoré, M., Lo Giudice, R., Marotta, R., Zuccato, E., 2004. Antibiotics in the environment: occurrence in italian stps, fate, and preliminary assessment on algal toxicity of amoxicillin. Environ. Sci. Technol. 38 (24), 6832–6838.

Ayrapetyan, M., Williams, T.C., Oliver, J.D., 2015. Bridging the gap between viable but non-culturable and antibiotic persistent bacteria. Trends Microbiol 23 (1), 7–13.

Bansal, O., 2019. Antibiotics in hospital effluents and their impact on the antibiotics resistant bacteria and remediation of the antibiotics: a review. Netw. Pharmacol. 4 (3–4), 6–30.
Barrette, W.C., Hannum, D.M., Wheeler, W.D., Hurst, J.K., 1989. General mechanism for the bacterial toxicity of hypochlorous acid: abolition of ATP production. Biochemistry 28 (23), 9172.
Besse, J.P., Garric, J., 2008. Human pharmaceuticals in surface waters: implementation of a prioritization methodology and application to the French situation. Toxicol. Lett. 176 (2), 104–123.
Bhowmick, G.D., Dhar, D., Nath, D., Ghangrekar, M.M., Banerjee, R., Das, S., Chatterjee, J., 2020. Coronavirus disease 2019 (COVID-19) outbreak: some serious consequences with urban and rural water cycle. npj Clean Water 3 (1), 32.
Cai, C., Kang, S., Xie, X., Liao, C., 2020. Ultrasound-assisted heterogeneous peroxymonosulfate activation with Co/SBA-15 for the efficient degradation of organic contaminant in water. J. Hazard. Mater. 385, 121519.
Cai, Y., Sun, T., Li, G., An, T., 2021. Traditional and emerging water disinfection technologies challenging the control of antibiotic-resistant bacteria and antibiotic resistance genes. ACS EST Eng. 1 (7), 1046–1064.
Carvalho, I.T., Santos, L., 2016. Antibiotics in the aquatic environments: a review of the European scenario. Environ. Int. 94, 736–757.
Casini, B., Baggiani, A., Totaro, M., Mansi, A., Costa, A.L., Aquino, F., Miccoli, M., Valentini, P., Bruschi, F., Lopalco, P.L., Privitera, G., 2018. Detection of viable but non-culturable legionella in hospital water network following monochloramine disinfection. J. Hosp. Infect. 98 (1), 46–52.
Chen, S., Li, X., Wang, Y., Jie, Z., Ye, C., Li, X., Guo, L., Zhang, S., Yu, X., 2018. Induction of *Escherichia coli* into a VBNC state through chlorination/chloramination and differences in characteristics of the bacterium between states. Water Res 142 (1), 279–288.
Daghrir, R., Drogui, P., 2013. Tetracycline antibiotics in the environment: a review. Environ. Chem. Lett. 11 (3), 209–227.
Daraei, H., Toolabian, K., Kazempour, M., Javanbakht, M., 2020. The role of the environment and its pollution in the prevalence of COVID-19. J. Infect. 81 (2), e168–e169.
Djordjevic, A., Spasic, S., Jovanovic-Galovic, A., Djordjevic, R., Grubor-Lajsic, G., 2004. Oxidative stress in diabetic pregnancy: SOD, CAT and GSH-Px activity and lipid peroxidation products. J. Maternal-Fetal Neo. M. 16 (6), 367–372.
Erental, A., Kalderon, Z., Saada, A., Smith, Y., Engelberg-Kulka, H., 2014. Apoptosis-like death, an extreme SOS response in. Escherichia coli e01426-01414.
Ghernaout, D., Elboughdiri, N., 2020. Antibiotics resistance in water mediums: background, facts, and trends. Appl. Eng. 4 (1), 1–6.
Guo, L., Wan, K., Zhu, J., Ye, C., Yu, X., 2020. Detection and distribution of vbnc/viable pathogenic bacteria in full-scale drinking water treatment plants. J. Hazard. Mater. 406 (4), 124335.
Gusarov, I., Nudler, E., 2005. NO-mediated cytoprotection: instant adaptation to oxidative stress in bacteria. Proc. Natl. Acad. Sci. 102 (39), 13855–13860.
Horn, S., Vogt, B., Pieters, R., Bouwman, H., Bezuidenhout, C., 2020. Impact of potential COVID-19 treatment on south african water sources already threatened by pharmaceutical pollution. Environ. Toxicol. Chem. 39 (7), 1305–1306.
Janion, C., 2001. Some aspects of the SOS response system–a critical survey. Acta Biochim. Pol. 48 (3), 599–610.
Jia, A., Hu, J., Wu, X., Peng, H., Wu, S., Dong, Z., 2011. Occurrence and source apportionment of sulfonamides and their metabolites in Liaodong Bay and the adjacent Liao River basin, North China. Environ. Toxicol. Chem. 30 (6), 1252–1260.
Jiang, Q., Yin, H., Li, G., Liu, H., An, T., Wong, P.K., Zhao, H., 2017. Elimination of antibiotic-resistance bacterium and its associated/dissociative blaTEM-1 and aac(3)-II antibiotic-resistance genes in aqueous system via photoelectrocatalytic process. Water Res. 125, 219–266.
Khan, M.H., Bae, H., Jung, J.-Y., 2010. Tetracycline degradation by ozonation in the aqueous phase: proposed degradation intermediates and pathway. J. Hazard. Mater. 181 (1), 659–665.
Klein, J.S., Lewinson, O., 2011. Bacterial ATP-driven transporters of transition metals: physiological roles, mechanisms of action, and roles in bacterial virulence. Metallomics 3 (11), 1098–1108.
Kovalakova, P., Cizmas, L., McDonald, T.J., Marsalek, B., Feng, M., Sharma, V.K., 2020. Occurrence and toxicity of antibiotics in the aquatic environment: a review. Chemosphere 251, 126351.
Kümmerer, K., 2009. Antibiotics in the aquatic environment – A review – Part I. Chemosphere 75 (4), 417–434.
Li, G., Liu, X., Zhang, H., An, T., Zhang, S., Carroll, A.R., Zhao, H., 2011. In situ photoelectrocatalytic generation of bactericide for instant inactivation and rapid decomposition of Gram-negative bacteria. J. Catal. 277 (1), 88–94.
Li, G., Liu, X., Zhang, H., Wong, P., An, T., Zhao, H., 2013. Comparative studies of photocatalytic and photoelectrocatalytic inactivation of *E. coli* in presence of halides. Appl. Catal. B-Environ. 140, 225–232.
Li, R., Williams, S.E., Li, Q., Zhang, J., Yang, C., Zhou, A., 2014. Photoelectrocatalytic degradation of ofloxacin using highly ordered TiO_2 nanotube arrays. Electrocatalysis 5 (4), 379–386.
Li, Y., Zhang, W., Niu, J., Chen, Y., 2012. Mechanism of photogenerated reactive oxygen species and correlation with the antibacterial properties of engineered metal-oxide nanoparticles. ACS Nano 6 (6), 5164–5173.
Lin, L., Su, Z., Li, Y., Zhang, C., 2021. Comparative performance and mechanism of bacterial inactivation induced by metal-free modified g-C_3N_4 under visible light: *escherichia coli* versus *Staphylococcus aureus*. Chemosphere 265, 129060.
Lindivat, M., Larsen, A., Hess-Erga, O.K., Bratbak, G., Hoell, I.A., 2020. Bioorthogonal non-canonical amino acid tagging combined with flow cytometry for determination of activity in aquatic microorganisms. Front. Microbiol. 11 https://doi.org/10.3389/fmicb.2020.01929.
Liu, D., Li, H., Gao, R., Zhao, Q., Yang, Z., Gao, X., Wang, Z., Zhang, F., Wu, W., 2021. Enhanced visible light photoelectrocatalytic degradation of tetracycline hydrochloride by I and P co-doped TiO_2 photoelectrode. J. Hazard. Mater. 406, 124309.
Ma, J., Zhou, H., Yan, S., Song, W., 2019. Kinetics studies and mechanistic considerations on the reactions of superoxide radical ions with dissolved organic matter. Water Res 149, 56–64.
Meng, N.C., Jin, B., Chow, C., Saint, C., 2010. Recent developments in photocatalytic water treatment technology: a review. Water Res. 44 (10), 2997–3027.
Merlin, C., Bonot, S., Courtois, S., Block, J.C., 2011. Persistence and dissemination of the multiple-antibiotic-resistance plasmid pB10 in the microbial communities of wastewater sludge microcosms. Water Res 45 (9), 2897–2905.
Mousset, E., Dionysiou, D.D., 2020. Photoelectrochemical reactors for treatment of water and wastewater: a review. Environ. Chem. Lett. 18 (4), 1301–1318.
Nie, X., Li, G., Gao, M., Sun, H., Liu, X., Zhao, H., Wong, P.K., An, T., 2014. Comparative study on the photoelectrocatalytic inactivation of *Escherichia coli* K-12 and its mutant *Escherichia coli* BW25113 using TiO_2 nanotubes as a photoanode. Appl. Catal. B Environ. 147, 562–570.
Pigeot-Remy, S., Simonet, F., Ailan, D., Lazzaroni, J.C., Guillard, C., 2012. Bactericidal efficiency and mode of action: a comparative study of photochemistry and photocatalysis. Water Res. 46 (10), 3208–3218.
Pu, Y., Li, Y., Xin, J., Tian, T., Fan, B., 2019. ATP-dependent dynamic protein aggregation regulates bacterial dormancy depth critical for antibiotic tolerance. Mol. Cell 73 (1), 143–156.
Qin, K., Zhao, Q., Yu, H., Xia, X., Li, J., He, S., Wei, L., An, T., 2021. A review of bismuth-based photocatalysts for antibiotic degradation: insight into the photocatalytic degradation performance, pathways and relevant mechanisms. Environ. Res. 199, 111360.
Qu, G., Li, X., Hu, L., Jiang, G., 2020. An imperative need for research on the role of environmental factors in transmission of novel coronavirus (COVID-19). Environ. Sci. Technol. 54 (7), 3730–3732.
Rodriguez-Rojas, A., Rodriguez-Beltran, J., Couce, A., Blazquez, J., 2013. Antibiotics and antibiotic resistance: a bitter fight against evolution. Int. J. Med. Microbiol. 303 (6–7), 293–297.
Schottroff, F., Fröhling, A., Zunabovic-Pichler, M., Krottenthaler, A., Schlüter, O., Jäger, H., 2018. Sublethal injury and viable but non-culturable (VBNC) state in microorganisms during preservation of food and biological materials by non-thermal processes. Front. Microbiol. 09 (11) https://doi.org/10.3389/fmicb.2018.02773.
Shi, H., Ni, J., Zheng, T., Wang, X., Wu, C., Wang, Q., 2020. Remediation of wastewater contaminated by antibiotics. A review. Environ. Chem. Lett. 18 (2), 345–360.
Shi, L., Liu, J., Gao, B., Sillanpää, M., 2022. Photoelectrocatalytic mechanism of PEDOT modified filtration membrane. Scien. Total Environ. 813, 152397.
Sun, H., Li, G., An, T., Zhao, H., Wong, P.K., 2016. Unveiling the photoelectrocatalytic inactivation mechanism of Escherichia coli: convincing evidence from responses of parent and anti-oxidation single gene knockout mutants. Water Res. 88, 135–143.
Sun, H., Li, G., Nie, X., Shi, H., Wong, P.K., Zhao, H., An, T., 2014. Systematic approach to in-depth understanding of photoelectrocatalytic bacterial inactivation mechanisms by tracking the decomposed building blocks. Environ. Sci. Technol. 48 (16), 9412–9419.
Sutton, M.D., Smith, B.T., Godoy, V.G., Walker, G.C., 2000. The SOS response: recent insights into umuDC-dependent mutagenesis and DNA damage tolerance. Annu. Rev. Genet. 34, 479–497.
Wang, J., Zhi, D., Zhou, H., He, X., Zhang, D., 2018. Evaluating tetracycline degradation pathway and intermediate toxicity during the electrochemical oxidation over a Ti/Ti_4O_7 anode. Water Res. 137 (6), 324–334.
Wang, J., Zhuan, R., 2020. Degradation of antibiotics by advanced oxidation processes: an overview. Sci. Total Environ. 701, 135023.
Wilke, B.C., Vidailhet, M., Favier, A., Guillemin, C., Ducros, V., Arnaud, J., Richard, M.J., 1992. Selenium, glutathione peroxidase (GSH-Px) and lipid peroxidation products before and after selenium supplementation. Clin. Chim. Acta 207 (1–2), 137–142.
Withers, H.R., 1975. Lethal and sublethal cellular injury in multifraction irradiation. Eur. J. Cancer 11 (8), 581–583.
Wu, S., Hu, Y.H., 2020. A comprehensive review on catalysts for electrocatalytic and photoelectrocatalytic degradation of antibiotics. Chem. Eng. J. 409 (10), 127739.
Ye, S., Chen, Y., Yao, X., Zhang, J., 2021. Simultaneous removal of organic pollutants and heavy metals in wastewater by photoelectrocatalysis: a review. Chemosphere 273, 128503.
Yin, H., Chen, X., Li, G., Chen, Y., Wang, W., An, T., Wong, P.K., Zhao, H., 2019. Sub-lethal photocatalysis bactericidal technology cause longer persistence of antibiotic-resistance mutant and plasmid through the mechanism of reduced fitness cost. Appl. Catal. B: Environ. 245, 698–705.
Yin, H., Chen, X., Li, G., Wang, W., Wong, P.K., An, T., 2021. Can photocatalytic technology facilitate conjugative transfer of ARGs in bacteria at the interface of natural sphalerite under different light irradiation? Appl. Catal. B: Environ. 287, 119977.
Yin, H., Li, G., Chen, X., Wang, W., An, T., 2020. Accelerated evolution of bacterial antibiotic resistance through early emerged stress responses driven by photocatalytic oxidation. Appl. Catal. B: Environ. 269, 118829.
Zhao, W., Yang, R., Shen, X., Zhang, S., Chen, X., 2013. Lethal and sublethal injury and kinetics of *Escherichia coli, Listeria monocytogenes* and *Staphylococcus aureus* in milk by pulsed electric fields. Food Control 32 (1), 6–12.